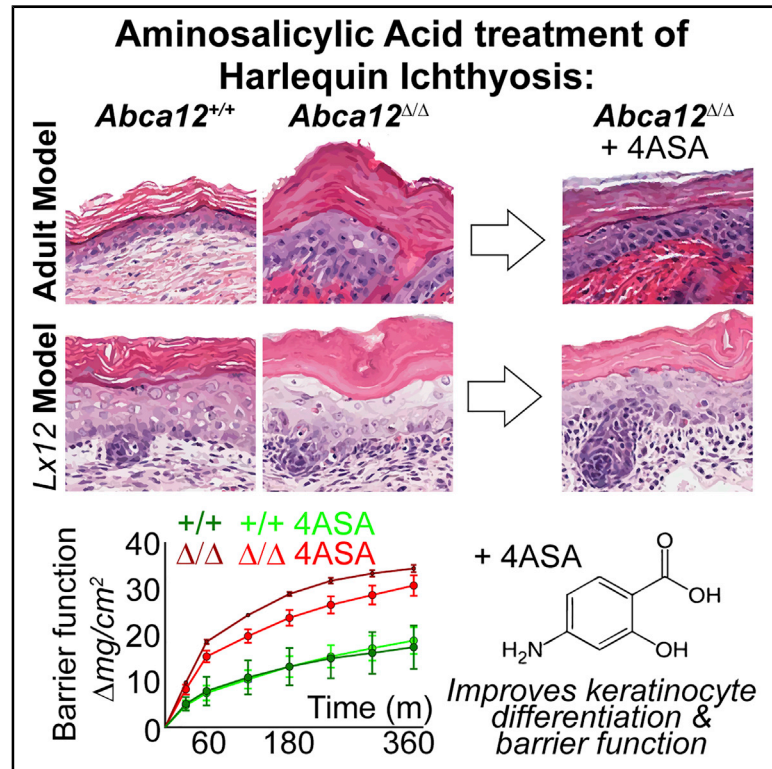**Article**

Topical Aminosalicylic Acid Improves Keratinocyte Differentiation in an Inducible Mouse Model of Harlequin Ichthyosis

Graphical Abstract

Authors

Denny L. Cottle, Gloria M.A. Ursino, Lynelle K. Jones, Ming Shen Tham, Allara K. Zylberberg, Ian M. Smyth

Correspondence

ian.smyth@monash.edu

In Brief

Harlequin ichthyosis arises because of the loss of lipid transport in the skin. Cottle et al. demonstrate that the treatment of mouse models of this disease with anti-inflammatory aminosalicylic acid drugs improves skin differentiation and protective barrier function.

Highlights

- Inflammation impairs keratinocyte differentiation and worsens harlequin ichthyosis

- Harlequin ichthyosis mice can be used to assess therapies for this disease

- Aminosalicylic acids may be therapeutic treatments for harlequin ichthyosis

- 4ASA improves skin differentiation and barrier function in harlequin ichthyosis models

CellPress

Article

Topical Aminosalicylic Acid Improves Keratinocyte Differentiation in an Inducible Mouse Model of Harlequin Ichthyosis

Denny L. Cottle,[1] Gloria M.A. Ursino,[1,2] Lynelle K. Jones,[1] Ming Shen Tham,[1] Allara K. Zylberberg,[1] and Ian M. Smyth[1,2,3,*]
[1]Department of Anatomy and Developmental Biology, Development and Stem Cell Program, Monash Biomedicine Discovery Institute (BDI), Monash University, Melbourne, Australia
[2]Department of Biochemistry and Molecular Biology, Monash University, Melbourne, Australia
[3]Lead Contact
*Correspondence: ian.smyth@monash.edu
https://doi.org/10.1016/j.xcrm.2020.100129

SUMMARY

Mutations in the lipid transport protein ABCA12 cause the life-threatening skin condition harlequin ichthyosis (HI), which is characterized by the loss of skin barrier function, inflammation, and dehydration. Inflammatory responses in HI increase disease severity by impairing keratinocyte differentiation, suggesting amelioration of this phenotype as a possible therapy for the condition. Existing treatments for HI are based around the use of retinoids, but their value in treating patients during the neonatal period has been questioned relative to other improved management regimens, and their long-term use is associated with side effects. We have developed a conditional mouse model to demonstrate that topical application of the aminosalicylic acid derivatives 5ASA or 4ASA considerably improves HI keratinocyte differentiation without the undesirable side effects of the retinoid acitretin and salicylic acid (aspirin). Analysis of changes in gene expression shows that 4ASA in particular elicits compensatory upregulation of a large family of barrier function-related genes, many of which are associated with other ichthyoses, identifying this compound as a lead candidate for developing topical treatments for HI.

INTRODUCTION

ABCA12 is a transmembrane transport protein thought to transfer intracellular lipids into secretory organelles called lamellar bodies, which in turn deposit them into the extracellular spaces between differentiating keratinocytes.[1] Patients with homozygous loss of function mutations in *ABCA12* develop harlequin ichthyosis (HI), a disease characterized by a defective cutaneous barrier lacking intercellular lipid layers, defects in desquamation, and associated dehydration and infection. Approximately 50% of HI neonates die, while survivors require frequent application of emollient creams to prevent dehydration and regular exfoliation to remove excess skin cells.[1–3] HI patients are often administered oral retinoids after birth to promote keratinocyte shedding; however, their value relative to improved management in the neonatal period has been questioned.[4]

We have previously profiled changes in gene expression in a mouse knockout model of HI, which highlighted an upregulation of pro-inflammatory markers.[5] By crossing these mice with animals ubiquitously expressing the anti-inflammatory protein IL-37b, several HI features were corrected.[5] Based on these studies, it was concluded that although inflammation does not directly contribute to defective barrier function, it plays a central role in disrupting the normal differentiation of the HI skin, worsening the appearance, severity, and progression of disease.[5,6]

This correction raised the possibility that other more clinically translatable anti-inflammatory compounds may represent potential new treatments for the condition. We were particularly interested in the prospect of re-purposing existing drugs to treat this ultra-rare condition. A search of the literature identified the aminosalicylic acid (ASA) family as one such potential therapy. 5ASA, also known as mesalamine and mesalazine, is already used in the treatment of inflammatory bowel disease (IBD) and has well-established safety profiles for topical application in the gut in high doses.[7,8] In addition, the drug is known to combat inflammation induced by ceramides,[9] which are a major component of the epidermal lipid barrier,[10] represent a potent inflammatory mediator,[11] and are one of the most dysregulated lipid species described in the HI epidermis.[6]

In this report, we detail the assessment of 5ASA and related compounds as candidate therapies for repurposing in the treatment of HI. Initial studies in the organ cultures of embryonic HI epidermis found that 5ASA significantly improves keratinocyte differentiation. We then developed an inducible mouse model of HI and tested the therapeutic effect of 5ASA, acitretin, and the related compounds 4ASA and aspirin (acetylsalicylic acid). These studies demonstrated that 4ASA provides superior improvement in cutaneous phenotypes compared to 5ASA, without the deleterious side effects observed following the application of acitretin or aspirin. Moreover, it corrects the

misexpression of numerous genes believed to contribute to barrier function and associated with other types of ichthyoses. These findings identify 4ASA as a candidate drug suitable for repurposing for the treatment of HI, an ultra-rare disease for which there is no current effective treatment.

RESULTS

5ASA Improves HI Embryonic Skin Differentiation *Ex Vivo*

To provide preliminary evidence for a protective effect of ASA in HI and to compare it with other drugs, we isolated embryonic (embryonic day 16.5 [E16.5]) back skin from *Abca12* null embryos (*Abca12^{lx12/lx12}*) and cultured them with 5ASA, ibuprofen and prednisolone. After 4 days, the skin from null embryos treated with carrier media alone showed profound differentiation defects, including abnormalities in the spinous layer, loss of granular layer, and thickening of the cornified envelope relative to wild-type siblings (Figure 1A). Differentiation markers were also altered, such that keratin 10 (KRT10) was absent and loricrin (LOR) was prematurely expressed in basal keratinocytes (Figures 1B and 1C). Ibuprofen proved toxic to all of the samples, with clear evidence of apoptosis and nuclear fragmentation in hematoxylin and eosin (H&E)-stained sections, while prednisolone had no obvious effect (Figures 1A and S1B). However, upon 5ASA treatment, HI skin showed less spinous layer abnormalities and a reduction in stratum corneum thickening compared to wild-type siblings, which showed no obvious drug-induced morphological change (Figure 1A). Patchy KRT10 expression was re-established in treated HI samples (Figure 1A), and LOR expression became enriched in the granular layer (Figure 1C). The expression of further differentiation markers involucrin (INV) and filaggrin (FLG) was restored in a manner analogous to KRT10 and LOR, respectively (Figures S1C and S1D). While *Abca12^{lx12/+}* mice are phenotypically normal, heterozygous embryo skins in this assay exhibited an intermediate phenotype that was also corrected by the application of 5ASA (Figures 1, S1C, and S1D). Based on these *in vitro* studies, we concluded that 5ASA shows considerable promise as a candidate HI therapy.

Development of *Abca12* Reporter and Conditional Strains

The neonatal lethality associated with the germline deletion of *Abca12*[12,13] precluded the testing or comparison of potential *in vivo* therapies for HI. To overcome this limitation, we developed a conditional model of this disease using *Abca12^{tm1a(EUCOMM)Hmgu}* gene trap embryonic stem cells, in which a LacZ cassette has been introduced upstream of a floxed exon (Figure 2A) (henceforth *Abca12^{tm1a}*). *Abca12^{tm1a/+}* mice exhibited LacZ expression in the upper layers of the epidermis (and to a lesser extent in the dermis and sebaceous glands), confirming the correct targeting of the *Abca12* gene (Figure 2B). Functional disruption of *Abca12* was also confirmed by generating E18.5 *Abca12^{tm1a/tm1a}* embryos, which developed HI phenotypes, exhibiting gross dysmorphology (Figure 2C), epidermal thickening, and failed granular layer compaction (Figure 2D), acquisition of expression of the wounding keratin KRT6a, expansion of KRT14, abnormal co-expression of

KRT14 and KRT10, and reduced periplakin (PPL) compaction (Figures 2E–2G).

The *Abca12^{tm1a}* mouse was used to derive a conditional *Abca12* allele (by Flp-mediated removal of the LacZ cassette), and mice were crossed with transgenic animals expressing a tamoxifen-activatable form of Cre specifically expressed in basal keratinocytes (*K14CreER*;[14] Figure S2A). HI was induced by the application of three topical doses of 1.5 mg tamoxifen analog 4-hydroxytamoxifen (4OHT), which resulted in the skin becoming dry and wrinkled in appearance over ~11 days (Figures 3A and 3B). PCR analysis of these *Abca12^{Δ/Δ}* mice showed that Cre recombinase was active only in mice administered 4OHT (Figure 3C). The skin of *Abca12^{Δ/Δ}* animals showed thickening of the epidermis, expansion of the stratum corneum (Figures 3D and S2B), loss of KRT10 expression, and induction of KRT6a (Figure 3E). Keratinocyte compaction in the granular layer was also impaired, with PPL expression more broadly distributed, while KRT14 expression persisted above the basal layer (Figure 3F). *Abca12^{Δ/Δ}* animals were predominantly culled 11 days after the induction of disease and demonstrated weight loss and a decline in health that we attributed to dehydration (Figure 3G). In some instances, mice were culled as early as 8 days post-induction if weight loss and health decline were more rapid. Disease development was profiled using a custom-made skin-related Nanostring GX array (see Data S1) which confirmed an ~50% loss of *Abca12* transcript and a reduction in *Abca1* mRNA consistent with previous reports (Figure 3H).[12] Using a previously characterized antibody,[15] no ABCA12 protein was detectable by immunofluorescence analysis, suggesting that the persistent transcript was non-functional (Figure 3I). Of the 95 genes included in the Nanostring array, 57 were found to be significantly dysregulated upon *Abca12* deletion, including the downregulation of differentiation markers (*Krt10* and *Lor*) and the upregulation of wounding and proliferation markers (*Krt5*, *Krt14*, *Krt6a/b*, and *Krt16*) (Data S1). Pathway analysis showed that the highest ranked MGI Mammalian Phenotype and Gene Ontology (GO) Biological Process terms were related to epidermal differentiation, lipid barrier function, and inflammation, which correlate with changes in the fetal skin of null mice[5] (Figures 3J and S2C). These changes mirror many of the hallmarks of human HI.

Intraperitoneal Injection of 5ASA

Having established an adult model of HI, we tested the effects of daily intraperitoneal (i.p.) injection of 5ASA. Mice were injected from days 5 to 10 and culled on day 11 or earlier as health dictated (Figure 4A). Injections were of a therapeutic dose determined to protect the mice from irradiation (25 mg/kg) or the maximum safe dose (125 mg/kg, determined to be half the median lethal dose [LD_{50}] dosage).[16] *Abca12^{f/f}* mice injected with 125 mg/kg 5ASA showed no adverse effects and gained weight over the 11-day experiment. In contrast, *Abca12^{Δ/Δ}* mice demonstrated a decline in weight, and the injection of 25 mg/kg 5ASA marginally increased this weight loss relative to vehicle injections (Figure 4B). A similar weight loss trend was seen for 125 mg/kg 5ASA-treated HI mice, although this was not statistically different. *Abca12^{f/f}* mice injected with 125 mg/kg 5ASA showed no morphological changes in their skin, while *Abca12^{Δ/Δ}*
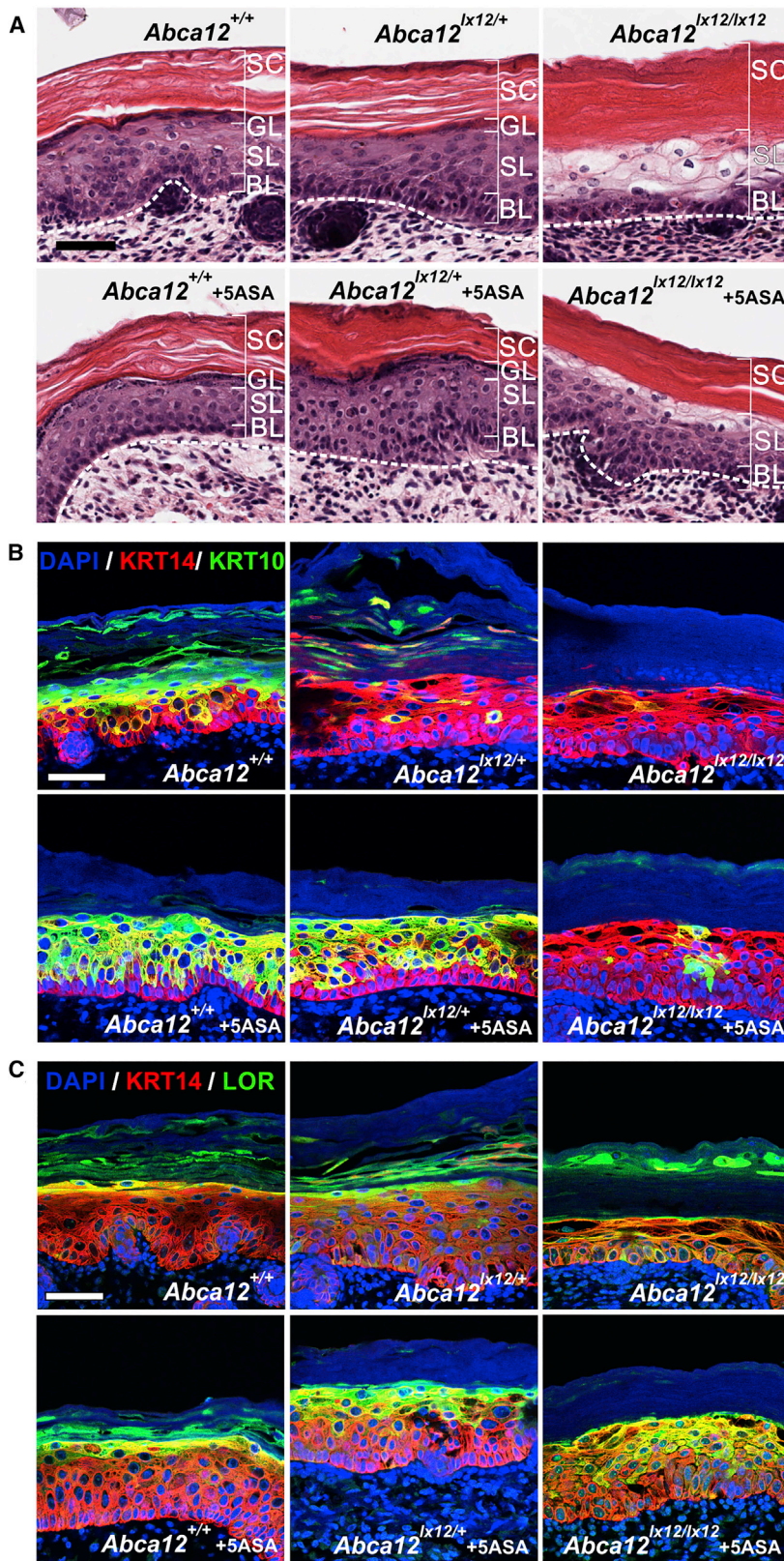
Figure 1. 5ASA Can Improve HI Embryonic Skin Differentiation

(A) Hematoxylin and eosin (H&E) staining of E16.5 *Abca12*$^{lx12/lx12}$ HI whole skin and control siblings, grown in an *ex vivo* whole-mount assay with 5ASA (n = 4–8). The phases of epidermal differentiation are indicated, as basal layer (BL), spinous layer (SL), granular layer (GL), and stratum corneum (SC). The dashed line marks the dermal boundary (excluding placodes).

(B and C) Immunostaining for keratin 14 (KRT14), keratin 10 (KRT10), and loricrin (LOR), counterstained with DAPI, as indicated.
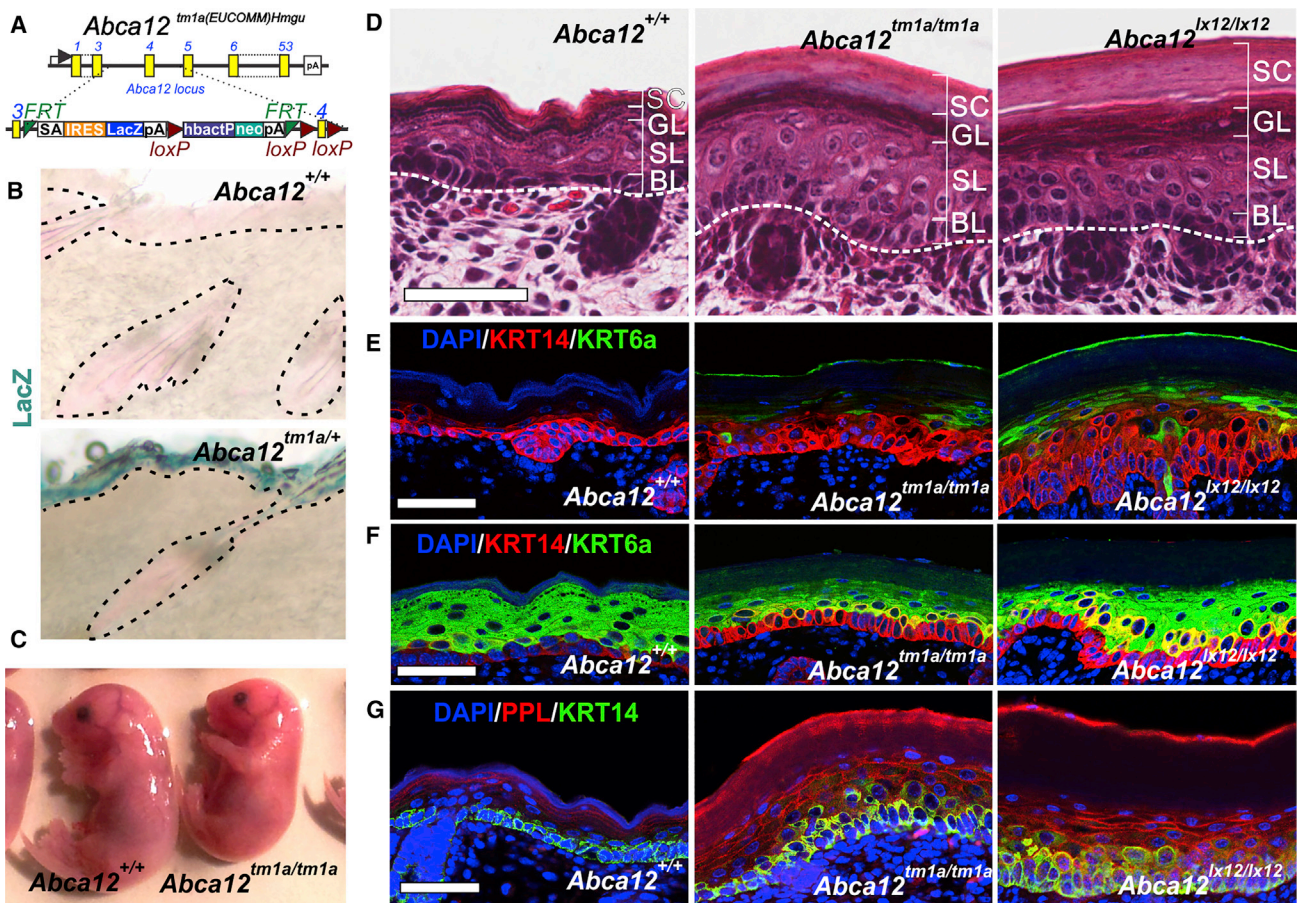
Scale bars, 50 μm.

Figure 2. Development of Abca12 Reporter Strain

(A) Schematic of $Abca12^{tm1a}$ targeting construct.

(B) LacZ staining of adult $Abca12^{tm1a/+}$ mouse skin and wild-type control to validate gene-trap targeting and expression (n = 3).

(C) E18.5 $Abca12^{tm1a/tm1a}$ embryos appeared smaller, with a shrink-wrapped, slightly redder, and less glossy appearance (n = 3).

(D) H&E staining of E18.5 wild-type (+/+), $Abca12^{tm1a/tm1a}$, and $Abca12^{lx12/lx12}$ skin (n = 3). The phases of epidermal differentiation are indicated, as BL, SL, granular layer GL, and SC. The dashed line marks the dermal boundary (excluding placodes).

(E–G) Immunostaining of E18.5 skins for keratin 6a (KRT6a), KRT14, KRT10, and periplakin (PPL), counterstained with DAPI, as indicated (n = 3).

Scale bars, 50 μm.

mice injected with either dosage of 5ASA demonstrated a reduction in epidermal thickness (~20%) relative to vehicle treatments (Figures 4C and 4D). Despite the modest skin thinning observed in HI mice with 5ASA injection, molecular phenotyping using Nanostring mRNA analysis showed only a few changes in gene expression (Figure 4E).

Topical ASA Creams Can Improve Adult HI Skin Differentiation

We hypothesized that the amount of active 5ASA reaching the skin through i.p. injection may be insufficient to realize significant improvements in phenotype. We therefore tested the effects of the daily topical application of 5ASA along with the retinoid acitretin and the related salicylic acids aspirin and 4ASA. We used Aveeno Dermexa moisturising cream (AD cream) as a vehicle for these studies to also ameliorate the barrier defects in our model system (Figure 5A). Animal cohorts were then monitored

for differences in survival, weight loss, salicylic acid excretion, skin histology, and gene expression. We initially studied the impact of AD cream alone on the HI phenotype. The proportion of HI mice that survived over time (as a function of ethical health limits) was used to provide an estimate of treatment tolerance. This analysis showed that AD cream-treated HI mice demonstrated slightly reduced survival relative to untreated HI mice (Figure 5B). Trinder assays[17] showed that treatments of HI mice with AD cream alone did not increase urine salicylic acid content (Figure 5C) relative to untreated mice, and while HI mice had a higher baseline urinary salicylic acid content, this is likely a secondary consequence of dehydration. AD cream alone did not change weight loss (Figure 5D), nor did it trigger obvious morphological changes in HI skin thickness (Figures 5E and 5F). While AD cream was tolerated by control mice, as measured by weight loss (Figure 5D), it caused modest skin thickening (Figure 5E), induced the wounding keratin KRT6a, and a led to a
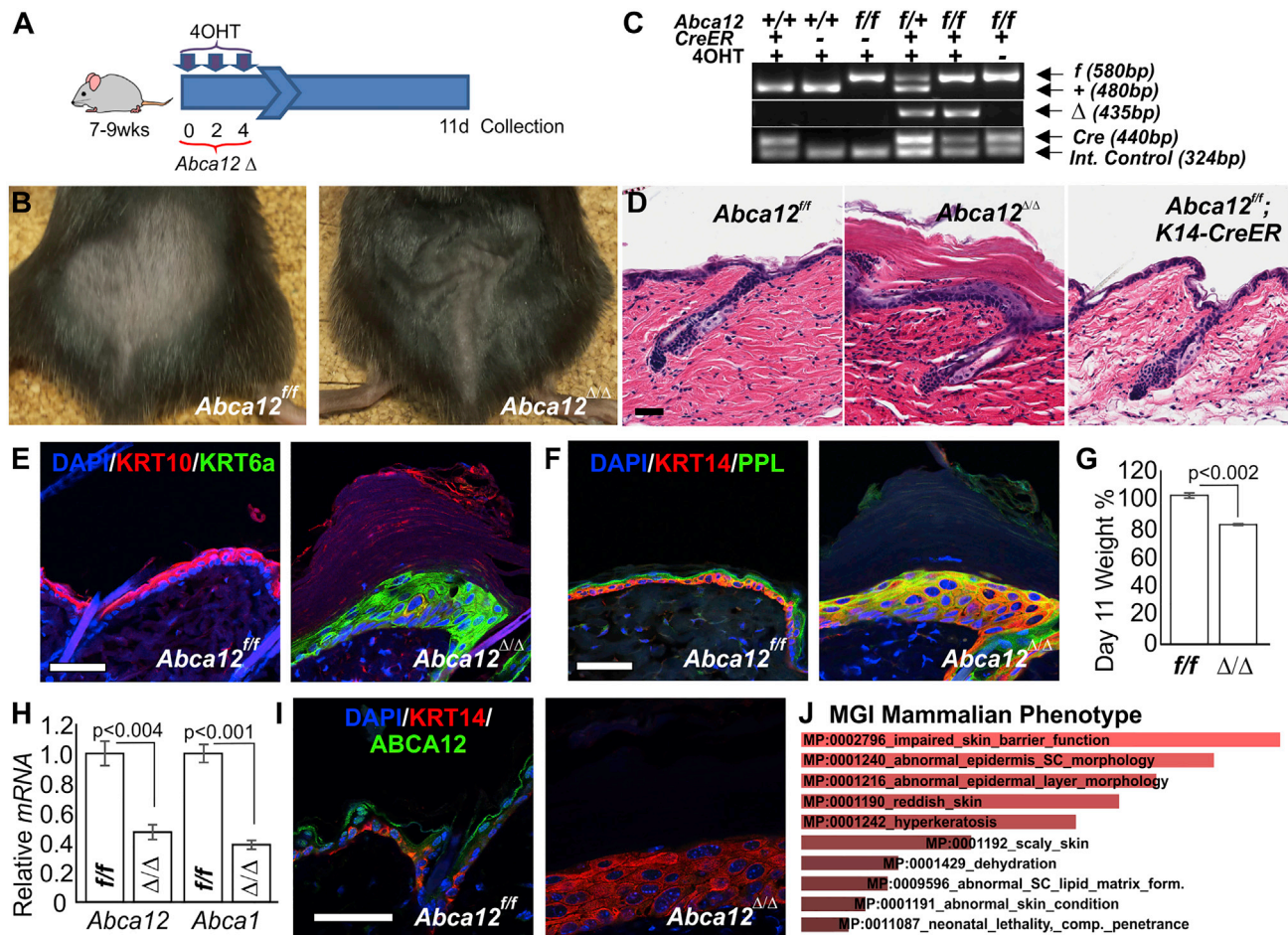
Figure 3. Development of *Abca12* Conditional Strain

(A) Overview of HI induction and experimental design.

(B) 4OHT treatment site of *Abca12^{f/f}* and *Abca12^{Δ/Δ}* mice.

(C) PCR analysis of Cre status, *Abca12* alleles, wild-type (+), floxed (f), and gene deletion (Δ) in *Abca12^{Δ/Δ}* mice and control genotypes (n = 3–4). Int., internal.

(D) H&E staining of *Abca12^{f/f}* and *Abca12^{Δ/Δ}* mice treated with 4OHT and *Abca12^{f/f} K14CreER* mice treated with acetone (n = 8).

(E) Immunostaining of skins for KRT6a, and KRT10, counterstained with DAPI, as indicated (n = 3).

(F) Immunostaining of skins for KRT14 and PPL, counterstained with DAPI, as indicated (n = 3).

(G) Day 11 body weight as a percentage of day 0 starting weight (n = 3–5). p values as indicated.

(H) Nanostring mRNA analysis of relative *Abca12* and *Abca1* expression in the epidermis of *Abca12^{tm1c/tm1c}* and *Abca12^{Δ/Δ}* mice (n = 3–5). p values as indicated.

(I) Immunostaining of skins for KRT14, and ABCA12, counterstained with DAPI, as indicated (n = 3).

(J) Top-ranked MGI Mammalian Phenotype terms from analysis of genes with significantly altered mRNA in *Abca12^{Δ/Δ}* mice.

All of the adult data are from day 11 of treatment. The error bars are SEMs. Scale bars, 50 μm.

slight impairment in keratinocyte compaction, and it had no impact on supra-basal KRT14 expression or reduced KRT10 expression compared to controls (Figures 5G and 5H).

We then examined mice treated with the retinoid acitretin, which is typically used to induce the shedding of excess skin layers apparent in HI infants at birth. HI mice treated with acitretin cream showed slightly worsened survival relative to the application of AD cream alone (Figure 5B), and it did not alter mouse weights relative to controls (Figure 5D). It reduced HI skin thickness by ∼20% (Figures 5E and 5F) and improved keratinocyte compaction as measured by PPL (Figure 5G). Somewhat paradoxically, acitretin reduced the expression of KRT10 but enhanced that of KRT6a (Figure 5H). In contrast, acitretin trig-gered epidermal thickening (Figures 5E and 5F) and a wounding response (Figure 5F), disrupted keratinocyte compaction (as indicated by PPL) (Figure 5G), reduced KRT10 expression, and induced KRT6a (Figure 5H) in control mice. These results suggest that while acitretin has some benefits in treating HI, it can severely disrupt normal epidermal homeostasis and induce disease.

Currently approved intestinal therapies introduce topical 5ASA concentrations into the colonic lumen at concentrations up to 100 mM.[18] Allowing for incomplete uptake, we therefore trialed 5ASA in AD cream at 3% and 6%, which equates to ∼196 and ∼392 mM, respectively. Even if the 6% dose was entirely in-gested by grooming, it would only equate to 240 mg/kg/day,
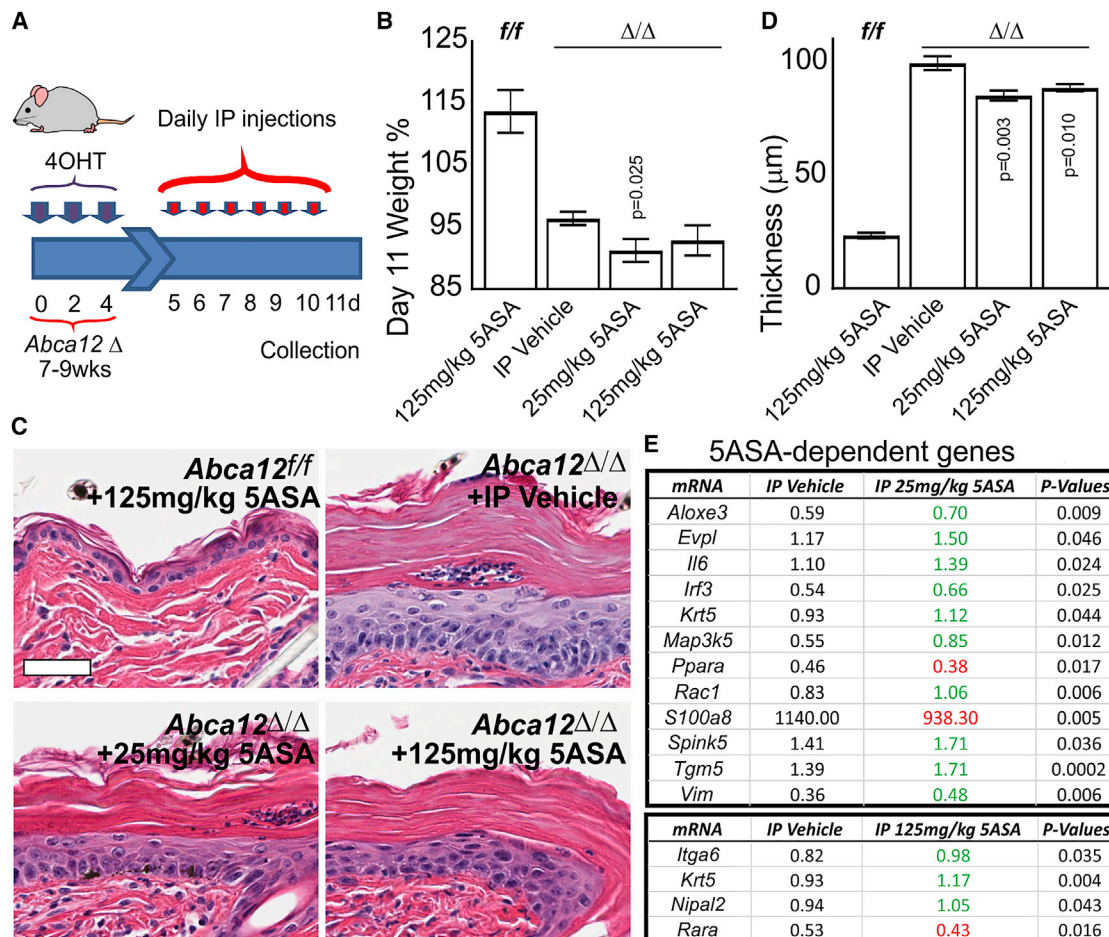
Figure 4. Intraperitoneal (i.p.) Injection of 5ASA
(A) Overview of experimental design.
(B) Day 11 body weight as a percentage of day 5 treatment starting weight (n = 5–6). The p value is relative to the vehicle-treated HI mice.
(C) H&E staining of *Abca12^Δ/Δ* and *Abca12^f/f* mice i.p. injected, as indicated (n = 5–6).
(D) Graph of the total epidermal thickness from treatments and genotypes indicated (n = 5–6). The p values are relative to the vehicle-treated HI mice.
(E) Tables reflect significantly changed genes from Nanostring mRNA analysis of epidermis taken at day 11. Expression levels are expressed relative to control *Abca12^f/f* untreated samples (defined as 1). Expression was normalized to the housekeeping gene *Edc3* (n = 3). The p values are relative to the vehicle-treated HI mice.
All of the mice are 4OHT treated and all of the data are from day 11 of treatment. The error bars are SEMs. Scale bars, 50 μm.

well below its oral LD$_{50}$ (3,370 mg/kg). Trinder assays suggested some minor absorption of topical 5ASA, although this was not to a statistically significant degree (Figure 5C). HI mice treated with 6% 5ASA cream showed a survival rate similar to that of AD cream-treated HI mice, while 3% 5ASA cream treatments were better tolerated (Figure 4B). Neither dose was able to arrest the weight loss in HI mice (Figure 5D). Only 3% 5ASA reduced epidermal thickness to a statistically significant extent (Figures 5E, 5F, and S3A), which was associated with a proportional thickness reduction in all skin layers, as well as improved keratinocyte compaction (Figures 5G and S3B). Unlike acitretin, 5ASA did not further reduce KRT10 expression (Figures 5H and S3C). These results indicate that 3% 5ASA treatment can thin and compact HI skin like acitretin without triggering further reductions in KRT10 or wounding responses. Therefore, we trialled a combination of 5ASA and acitretin (combination cream), but

this had the worst survival rate among HI treatments, increased weight loss, and exhibited no additive or synergistic effects compared to either drug alone (Figures 5, S3, and S4).

We next investigated the therapeutic effects of two structural analogs of 5ASA: aspirin and 4ASA. Survival in aspirin-treated HI cohorts was similar to that of AD cream-treated mice (Figure 5B), was not systemically absorbed (Figure 5C), and did not alter animal weights (Figure 5D) or reduce HI epidermal thickness (Figures 5E and 5F). However, it did cause blistering and wounding (Figure 5F), especially evident in control mice, which developed an ichthyosis-like condition, exhibited impaired keratinocyte compaction, upregulated KRT6a, and reduced KRT10 (Figures 5E–5H). In contrast, 4ASA cream-treated HI mice demonstrated survival equivalent to or better than AD cream-treated cohorts (Figure 5B) and was not systemically absorbed (Figure 5C). Notably 1.5% 4ASA cream was the only treatment
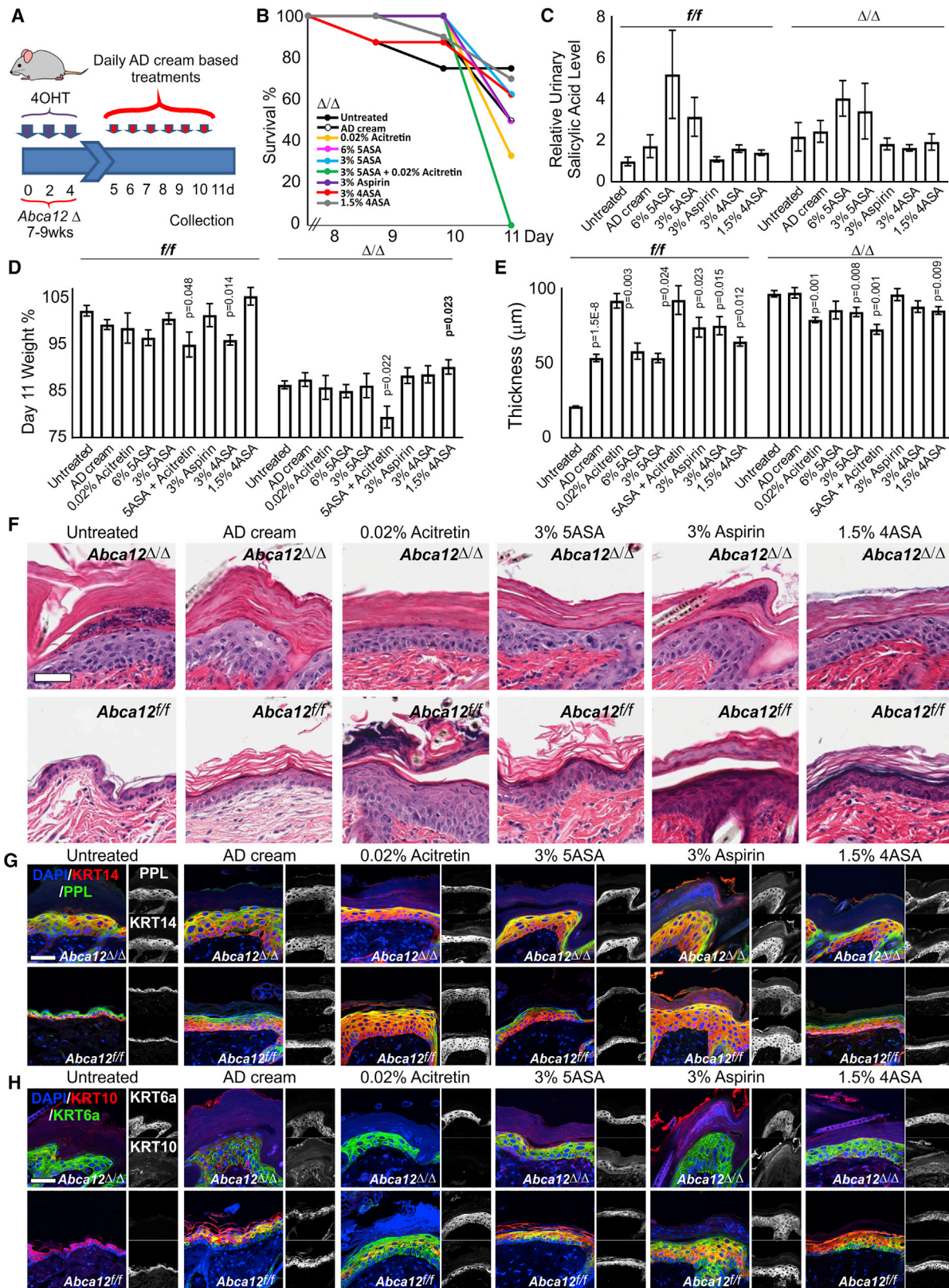
(legend on next page)

that was able to attenuate weight loss in HI mice (Figure 5D). Application of both 1.5% and 3% 4ASA reduced epidermal thickness relative to AD cream controls (Figures 5E, 5F, and S3A) and improved keratinocyte compaction (Figures 5G and S3B). As with 5ASA treatments, KRT10 and KRT6a immunostaining profiles were unchanged (Figures 5H and S3C). The application of 1.5% 4ASA had minor effects on control mice, with some skin thickening, while 3% 4ASA caused weight loss and a further thickened epidermis (Figures 5D–5F and S3A–S3C).

Based on these experiments, we conclude that 1.5% 4ASA represents the most promising treatment for HI identified in this study as it shares the beneficial properties of 3% 5ASA in correcting skin morphology without the detrimental side effects of acitretin. Moreover, it was the only treatment tested that was able to counter the weight loss normally observed in HI mouse models and did not demonstrate systemic absorption.

Molecular Profiling of Disease Rescue

To gain a better understanding of the molecular effects of each treatment, we performed Nanostring mRNA analysis using untreated *Abca12* $^{f/f}$ mice as controls. Heatmap clustering of expression profiles (based on elucidean distance) demonstrated that control mice treated with AD cream alone, 1.5% 4ASA, 6% 5ASA, and 3% 5ASA (treatments with minor morphological effects) grouped together near untreated control mice, while control mice treated with 3% 4ASA, combination, 3% aspirin and 0.02% acitretin (treatments causing skin thickening) clustered together in a group with HI mice. Of all of the HI treatments, 1.5% 4ASA brought the gene profile closest to the baseline state based on Elucidean distance (Figure 6A).

While 3% 5ASA and 0.02% acitretin treatments demonstrated similar morphological outcomes in HI mice, there was little overlap in gene signatures and analysis of expression changes following combination cream treatment, which suggested that these compounds were partially antagonistic (Figure 6B). There were few shared gene expression changes between 3% aspirin and the related compounds 5ASA and 4ASA, while all of the salicylic acids had only minor overlap with acitretin (Figure 6C). Interestingly, 6% 5ASA and 3% 5ASA appeared to activate distinct genes, which is consistent with the observed differences in disease rescue. The beneficial effects of the lower dose mirrored the gene expression changes that were observed following treatments with either concentration of 4ASA (Figure 6D). Consistent with their worsening of disease phenotypes,

aspirin and acitretin induced gene expression changes that were similar to those observed in HI itself (Figure 6E). Ingenuity Pathway Analysis (IPA) downstream prediction analysis[19] also found that 1.5% 4ASA treatments modified gene sets likely to associate with reduced neonatal death and reduced keratinocyte proliferation, as well as those related to increased development, growth, and differentiation of epithelia tissue, steroid quantity, and cholesterol and sterols concentrations (Figure 6F). Perhaps owing to the small number of inflammatory genes in our Nanostring panel, IPA analysis did not predict a reduction in inflammation from 1.5% 4ASA treatment and inflammatory *Ccl17*, *Cxcl1*, *Il-1a*, *Il-6*, *Il19*, and *Tnfa* mRNA species appeared upregulated (Data S1). To further analyze how 1.5% 4ASA alters inflammatory responses we used a RayBiotech Quantibody Mouse Inflammation Q1 Array to analyze 40 common inflammatory factors at the protein level from skin extracts. Most protein factors, including C-X-C motif ligand 1 (CXCL1), interleukin-1α (IL-1α), IL-6, and tumor necrosis factor α (TNF-α), in the array did not demonstrate significant changes upon 4ASA treatment. However, CCL1 and CCL17 proteins were significantly downregulated by 1.5% 4ASA relative to AD cream and untreated samples, respectively (Figure 6G), thereby confirming that 4ASA has anti-inflammatory actions.

Nanostring mRNA analysis also demonstrated that 1.5% 4ASA cream had the most efficacy, promoting the upregulation of 33 genes known to positively contribute to keratinocyte differentiation, waterproofing, and lipid barrier formation. Notably, many of these result in ichthyosis when they are mutated (e.g., *Aloxe3*, *Alox12b*, *Cers3*, *Cyp4f22*, *Gba*, *Grhl3*, *Lipn*, *Nipal4*, *Pnpla1*, and *Tgm1*), and several lipid- and differentiation-regulating transcription factors were also elevated (e.g., *Fabp5*, *Cebpa*, *Ppard*, *Rara*, and *Rxra*; Figure 6H; Data S1). The upregulation of these genes suggested that an improvement in barrier function may explain the reduction of weight loss in cohorts of mice treated with 1.5% 4ASA. To formally examine this possibility, we performed transepidermal water loss (TEWL) assays on E16.5 *Abca12* ^{Ix12} skin cultured with 10 mM 4ASA for 4 days. This treatment realized a similar improvement in skin morphology as 5ASA (Figures 1A and 6I) and improved barrier function, significantly preventing disease-associated dehydration in the TEWL assay (Figure 6J). This suggests that topical 1.5% 4ASA realizes the best normalization of gene expression relative to control mice, as well as acting to positively regulate the transcription of many genes associated with cutaneous barrier function.

Figure 5. Topical ASA Creams Can Improve Adult HI Skin Differentiation

(A) Overview of experimental design.

(B) Survival percentage graph based on health-euthanasia thresholds as an estimate of treatment tolerance (n = 3–10).

(C) Relative urine salicylic acid content from topical treatments determined from Trinder assay (n = 3–5).

(D) Day 11 body weight as a percentage of day 5 treatment starting weight (n = 3–9); unbolded. The p values are relative to the AD cream-treated mice of matched genotype, while bolded p values are relative to the untreated mice of the matched genotype.

(E) Graph of the total epidermal thickness from treatments and genotypes indicated (n = 3–12). The p values are relative to the AD cream-treated mice of the matched genotype, with the exception of the AD cream itself, which is relative to the untreated mice.

(F) H&E staining of *Abca12*$^{Δ/Δ}$ and *Abca12*$^{f/f}$ mice treated with AD creams as indicated (n = 3–8).

(G) Immunostaining of *Abca12*$^{Δ/Δ}$ and *Abca12*$^{f/f}$ skins (treated as indicated) for KRT14 and/or PPL counterstained with DAPI, as indicated (n = 3–5).

(H) Immunostaining of *Abca12*$^{Δ/Δ}$ and *Abca12*$^{f/f}$ skins (treated as indicated) for KRT10 and/or KRT6a counterstained with DAPI, as indicated (n = 3–5).

All data are from day 11 of treatment. All of the mice are 4OHT treated unless indicated. 5ASA + acitretin refers to 3% 5ASA + 0.02% combination acitretin treatment. The error bars are SEMs. Scale bars, 50 μm.
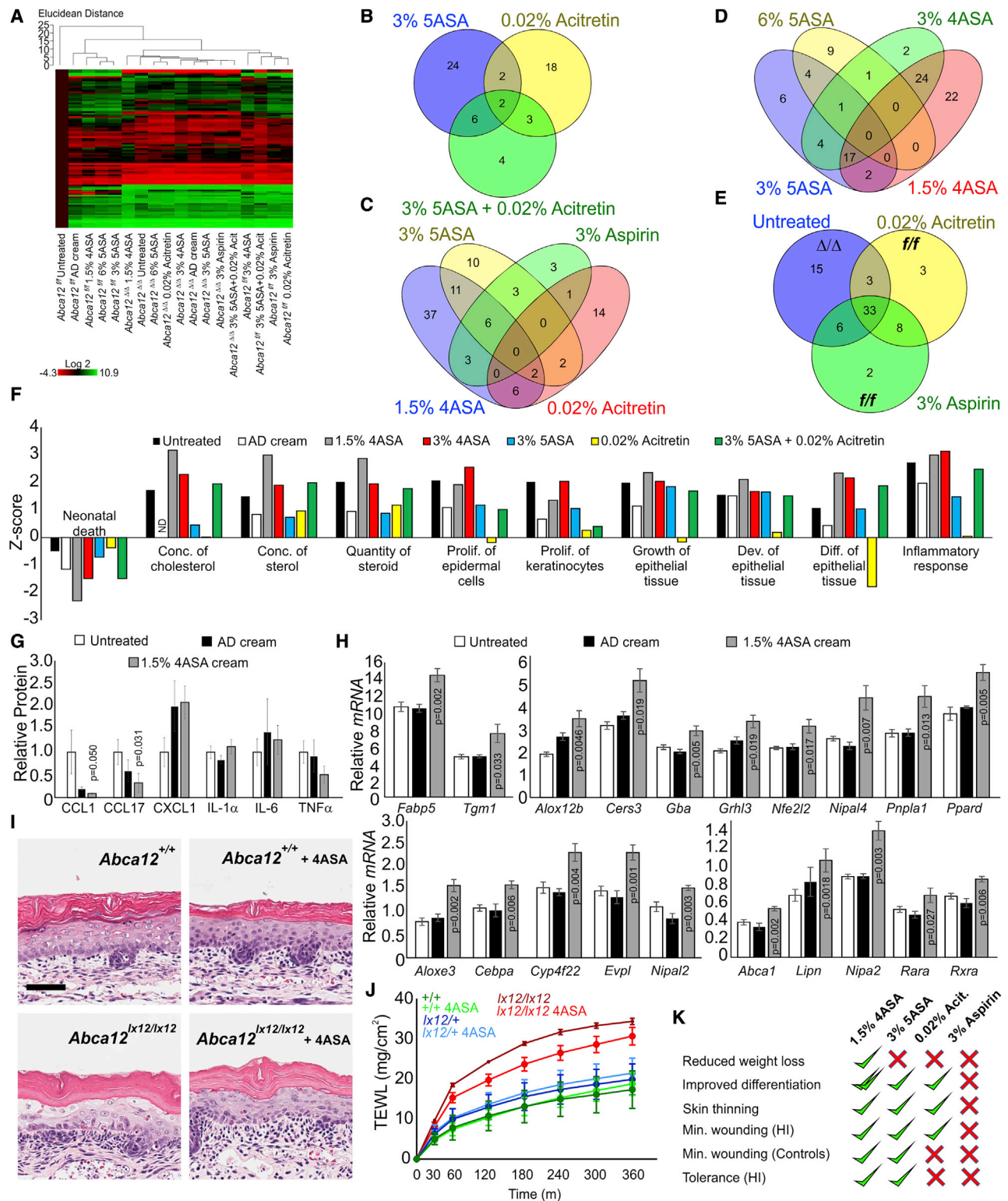
Figure 6. Analysis of the Molecular Impacts of Drug Treatment

(A) Heatmap of mRNA expression profiles from Nanostring analysis of all treatments (n = 4–6).

(B) Comparison of common mRNA changes between 3% 5ASA, 0.02% acitretin, and 3% 5ASA + 0.02% acitretin cream treatments of Abca12$^{\Delta/\Delta}$ mice.

(C) Comparison of common mRNA changes between 3% 5ASA, 3% aspirin, 1.5% 4ASA, and 0.02% acitretin cream treatments of Abca12$^{\Delta/\Delta}$ mice.

(legend continued on next page)

DISCUSSION

In this study, we profiled a selection of anti-inflammatory compounds as treatments for HI, identifying 4ASA as a leading candidate for further clinical development. The initial studies on cultured skin found that prednisolone treatment did not elicit beneficial effects, which is consistent with previous reports that corticosteroids are ineffective in treating HI.[20] To test alternate therapies *in vivo*, we developed an inducible mouse model with the morphological and molecular hallmarks of HI. Initial testing of 5ASA administered systemically demonstrated only modest improvement within the safe dosage limits, and a topical delivery strategy was pursued. While the use of AD cream as a topical base was predominantly neutral, it slightly reduced survival in HI animals (Figures 5B and S4) and increased skin thickening and signs of impaired differentiation and wounding in control animals (Figures 5 and S4; Data S1). Based on these findings, further work is required to define a suitable carrier for the efficacious HI treatments identified in this study.

In testing a panel of candidate drugs using these mice, we have shown that the topical application of 5ASA and 4ASA can improve HI keratinocyte differentiation, with the latter compound demonstrating superior efficacy at lower concentrations. This drug has the added advantage that it upregulates an extensive network of essential skin barrier genes mutated in other ichthyoses; therefore, it will be of interest to examine its potential therapeutic use in a range of related skin conditions. Its efficacy appears to lie, at least in part, in the promotion of differentiation and lipid production at the expense of keratinocyte proliferation, as well as in reducing CCL1- and CCL17-driven inflammatory responses. These finding correlate with previous work demonstrating the ability of 5ASA to reduce CCL17 inflammatory responses in the skin.[21]

Despite its structural similarity to ASAs, aspirin did not proportionally thin the HI epidermis but instead induced an ichthyosis-like condition in control animals. We note that the aspirin precursor salicylic acid is extensively used in skin products as a chemical exfoliant, which may account for the blistering and wounding observed. Full-body topical application of salicylic acid in HI patients is known to cause systemic toxicity.[22] In contrast, however, 4ASA and 5ASA have been used in clinical trials to topically treat psoriasis with no toxic effects.[23,24] Extrapolation of the doses used in this study to full-body coverage would be well below those that trigger salicylic acid poisoning, as the LD_{50} of 4ASA is ~8-fold less than that of salicylic acid. Trinder

assays of mouse urine did not detect increases in urinary salicylic acid levels for any treatment (Figure 5C), suggesting that the risk of salicylic acid poisoning from topical 4ASA is low.

Reye syndrome is a rare condition that may arise secondary to viral infections in young patients using aspirin, and is potentially linked to altered fatty acid metabolism in the liver.[25,26] Both 4ASA and 5ASA are structurally similar to aspirin and can have liver toxicity,[27,28] so some caution is warranted when considering their use in treating HI. However, children with IBD are prescribed 5ASA and 4ASA as a treatment for tuberculosis (TB) at dosages similar to adults,[29,30] and neither of these regimens has been linked to Reye syndrome. A further study of pregnant mothers taking 5ASA also showed that the drug was considered safe.[7] Taken together with our findings of limited systemic uptake of topically applied ASAs, this suggests that the relatively low risk of developing Reye syndrome would be outweighed by the significant benefits achieved from the treatment of HI children.

The current treatments for HI patients are based around regimens of frequent bathing, exfoliation, and application of emollient creams.[1–3] Retinoids like acitretin are orally prescribed for many skin conditions to promote desquamation, and retrospective analysis suggests that they may improve survival outcomes in HI infants.[31] However, their value in treating HI neonates has been questioned on the basis that improvements in survival associated with their use could be attributed to more active neonatal management regimens.[4] The long-term use of retinoids is further complicated by the potential for serious side effects. Here, we demonstrate that while acitretin treatment does promote modest improvements in epidermal thickness, it was also capable of inducing an ichthyosis-like phenotype. In contrast, 5ASA and the lower dose of 4ASA were relatively safe for control animals and both compounds have well-established safety profiles determined from patient trials to treat IBD, TB, and psoriasis.[7,8,23,24,32]

Our work raises the question of how ASA treatment results in improved epidermal differentiation in HI. While there is no clear mechanism evident from our analysis of gene expression, 5ASA has been reported to act as a peroxisome proliferator-activated receptor γ (PPARγ) agonist and to reduce PPARδ activity.[33,34] The PPARs are potent regulators of epidermal differentiation,[35,36] and we found that *Ppard*, *Pparg*, and/or the heterodimeric receptor partner, *Rxra*, were almost always altered in our gene arrays. The partial antagonism observed between the 5ASA and acitretin combination treatment supports a common

---

(D) Comparison of common mRNA changes between 6% 5ASA, 3% 5ASA, 3% 4ASA, and 1.5% 4ASA cream treatments of *Abca12$^{Δ/Δ}$* mice.

(E) Comparison of common mRNA changes between *Abca12$^{Δ/Δ}$* mice and *Abca12$^{f/f}$* mice treated with 3% aspirin and 0.02% acitretin cream treatments.

(F) IPA downstream predictions following 1.5% 4ASA treatments of *Abca12$^{Δ/Δ}$* mice.

(G) Relative protein expression levels of chemokines and cytokines indicated from Inflammatory array analysis of whole-skin protein extracts. The p value for CCL1 is relative to the AD cream-treated samples, while the p value for CCL17 is relative to untreated.

(H) Significantly changed mRNA expression from Nanostring analysis of untreated AD cream and 1.5% 4ASA-treated *Abca12$^{Δ/Δ}$* epidermis (n = 5). The p values are relative to AD cream, except for *Lipn*, which is relative to untreated.

(I) H&E staining of E16.5 *Abca12$^{+/+}$* and *Abca12$^{lx12/lx12}$* HI whole skin grown in an *ex vivo* whole-mount assay without and with 10 mM 4ASA (n = 5).

(J) TEWL assays of E16.5 *Abca12^{lx12}* litter skins grown in an *ex vivo* whole-mount assay without and with 4ASA (n = 3–8). The p values for time-matched pairs of *Abca12$^{lx12/lx12}$* skins without and with 4ASA (upper 2 arcs) are p = 0.038 (60 min), p = 0.019 (120 min), p = 0.021 (180 min), p = 0.027 (240 min), and p = 0.047 (300 min).

(K) Summary of topical treatment efficacy.

All of the topical treatment data are from day 11 of treatment, and all of the mice are 4OHT treated, unless indicated. The error bars are SEMs. Scale bars, 50 μm.

action via retinoic acid-related pathways, which compete with PPARs for binding to RXRs.

In conclusion, we have developed an inducible model of HI that has allowed us to trial ASAs as potential treatments of this disease and to benchmark their actions against existing retinoid treatments (Figure 6K). These studies have shown that 1.5% 4ASA can promote keratinocyte differentiation and improve lipid barrier function in HI animals, with only minor effects on control mice. The challenge remains to determine the best vehicle for delivering ASAs effectively to HI patients in a manner that best restores barrier function. We propose that the most effective and promising treatment for this lifelong, highly morbid disease will be to formulate 4ASA into a skin cream base specifically engineered to the unique waterproofing and sensitivity needs of people with this disease.

Limitations of Study

We provide evidence for a therapeutic effect of ASAs in countering inflammatory phenotypes associated with HI. While the improvements in skin differentiation and function in 4ASA-treated animal models of this disease were encouraging, the long-term benefits of 4ASA could not be assessed due to a decline in the health of HI animals. We attribute this decline to the persistence of the barrier function defects associated with the abnormal deposition of lipids in the skin of these mice. For this reason, measuring the effects of long-term treatment with 4ASA will require the co-development of a suitable waterproofing carrier cream. There are also caveats in the use of animal models to examine the biology of this disease. While many of the effects of the loss of *Abca12* are shared between HI patients and our mice, there remain obvious differences in the biology of the epidermis in the two species, meaning that the extent of rescue in patients may differ. Moreover, cutaneous phenotypes in HI patients develop over a longer time course and likely involve inflammatory responses directed in part by the environmental challenges to which an individual is exposed. In the case of our mice, the induction of disease is relatively rapid, and the animals exist in a pathogen-controlled and highly stable environment. These differences may ultimately have an impact on the effectiveness of 4ASA and related compounds in ameliorating disease phenotypes in HI patients.

STAR★METHODS

Detailed methods are provided in the online version of this paper and include the following:

- KEY RESOURCES TABLE
- RESOURCE AVAILABILITY
  - Lead Contact
  - Materials Availability
  - Data and Code Availability
- EXPERIMENTAL MODEL AND SUBJECT DETAILS
- METHOD DETAILS
  - Genotyping
  - Embryonic skin culture
  - Tamoxifen induction of HI
  - 5ASA intraperitoneal injection

- Topical application of creams
- Assay of urine salicylic acid content
- Histological Analysis and Microscopy
- Antibodies and immunostaining
- Nanostring mRNA Analysis
- Inflammatory Array
- Transepidermal water loss assays
- QUANTIFICATION AND STATISTICAL ANALYSES

AUTHOR CONTRIBUTIONS

D.L.C. co-designed the project, performed the data acquisition and analysis, and wrote the manuscript. G.M.A.U., L.K.J., A.K.Z., and M.S.T. contributed to data acquisition. I.M.S. co-designed the project, supervised, mentored, and edited the manuscript.

DECLARATION OF INTERESTS

D.L.C., G.M.A.U., and I.M.S. are inventors on patent applications WO 2016/145488 A1, PCT/AU2016/050185, US 15/557405, India 201727036282, Europe 16764064.8, Australia 2016232987, Canada 2984949, Japan 2017-549008, and China 201680028353.X, related to ASA treatment of ichthyosis skin diseases and received funding from Factor Therapeutics under a research collaboration and option agreement.

REFERENCES

1. Oji, V., and Traupe, H. (2009). Ichthyosis: clinical manifestations and practical treatment options. Am. J. Clin. Dermatol. *10*, 351–364.

2. Cambazard, F., Haftek, M., Hermier, C., Lachaud, A., Dutruge, J., Gallet, S., Armand, J.P., Staquet, M.J., and Thivolet, J. (1988). [Harlequin fetus treated with etretin (RO 10-1670)]. Ann. Dermatol. Venereol. *115*, 1128–1130.

3. Singh, S., Bhura, M., Maheshwari, A., Kumar, A., Singh, C.P., and Pandey, S.S. (2001). Successful treatment of harlequin ichthyosis with acitretin. Int. J. Dermatol. *40*, 472–473.

4. Milstone, L.M., and Choate, K.A. (2013). Improving outcomes for harlequin ichthyosis. J. Am. Acad. Dermatol. *69*, 808–809.

5. Cottle, D.L., Ursino, G.M., Ip, S.C., Jones, L.K., Ditommaso, T., Hacking, D.F., Mangan, N.E., Mellett, N.A., Henley, K.J., Sviridov, D., et al. (2015). Fetal inhibition of inflammation improves disease phenotypes in harlequin ichthyosis. Hum. Mol. Genet. *24*, 436–449.

6. Ip, S.C.I., Cottle, D.L., Jones, L.K., Weir, J.M., Kelsell, D.P., O'Toole, E.A., Meikle, P.J., and Smyth, I.M. (2017). A profile of lipid dysregulation in harlequin ichthyosis. Br. J. Dermatol. 177, e217–e219.

7. Diav-Citrin, O., Park, Y.H., Veerasuntharam, G., Polachek, H., Bologa, M., Pastuszak, A., and Koren, G. (1998). The safety of mesalamine in human pregnancy: a prospective controlled cohort study. Gastroenterology 114, 23–28.

8. Fabro, S. (1978). Penetration of chemicals into the oocyte, uterine fluid, and preimplantation blastocyst. Environ. Health Perspect. 24, 25–29.

9. Kaiser, G.C., Yan, F., and Polk, D.B. (1999). Mesalamine blocks tumor necrosis factor growth inhibition and nuclear factor kappaB activation in mouse colonocytes. Gastroenterology 116, 602–609.

10. Takagi, Y., Nakagawa, H., Matsuo, N., Nomura, T., Takizawa, M., and Imokawa, G. (2004). Biosynthesis of acylceramide in murine epidermis: characterization by inhibition of glucosylation and deglucosylation, and by substrate specificity. J. Invest. Dermatol. 122, 722–729.

11. Barber, S.A., Detore, G., McNally, R., and Vogel, S.N. (1996). Stimulation of the ceramide pathway partially mimics lipopolysaccharide-induced responses in murine peritoneal macrophages. Infect. Immun. 64, 3397–3400.

12. Smyth, I., Hacking, D.F., Hilton, A.A., Mukhamedova, N., Meikle, P.J., Ellis, S., Satterley, K., Collinge, J.E., de Graaf, C.A., Bahlo, M., et al. (2008). A mouse model of harlequin ichthyosis delineates a key role for Abca12 in lipid homeostasis. PLoS Genet. 4, e1000192.

13. Yanagi, T., Akiyama, M., Nishihara, H., Sakai, K., Nishie, W., Tanaka, S., and Shimizu, H. (2008). Harlequin ichthyosis model mouse reveals alveolar collapse and severe fetal skin barrier defects. Hum. Mol. Genet. 17, 3075–3083.

14. Vasioukhin, V., Degenstein, L., Wise, B., and Fuchs, E. (1999). The magical touch: genome targeting in epidermal stem cells induced by tamoxifen application to mouse skin. Proc. Natl. Acad. Sci. USA 96, 8551–8556.

15. Ursino, G.M., Fu, Y., Cottle, D.L., Mukhamedova, N., Jones, L.K., Low, H., Tham, M.S., Gan, W.J., Mellett, N.A., Das, P.P., et al. (2020). ABCA12 regulates insulin secretion from β-cells. EMBO Rep. 21, e48692.

16. Sudheer Kumar, M., Unnikrishnan, M.K., and Uma Devi, P. (2003). Effect of 5-aminosalicylic acid on radiation-induced micronuclei in mouse bone marrow. Mutat. Res. 527, 7–14.

17. Trinder, P. (1954). Rapid determination of salicylate in biological fluids. Biochem. J. 57, 301–303.

18. Williams, C., Panaccione, R., Ghosh, S., and Rioux, K. (2011). Optimizing clinical use of mesalazine (5-aminosalicylic acid) in inflammatory bowel disease. Therap. Adv. Gastroenterol. 4, 237–248.

19. Krämer, A., Green, J., Pollard, J., Jr., and Tugendreich, S. (2014). Causal analysis approaches in ingenuity pathway analysis. Bioinformatics 30, 523–530.

20. Fleckman, P. (2003). Management of the ichthyoses. Skin Therapy Lett. 8, 3–7.

21. Goldie, S.J., Cottle, D.L., Tan, F.H., Roslan, S., Srivastava, S., Brady, R., Partridge, D.D., Auden, A., Smyth, I.M., Jane, S.M., et al. (2018). Loss of GRHL3 leads to TARC/CCL17-mediated keratinocyte proliferation in the epidermis. Cell Death Dis. 9, 1072.

22. Ward, P.S., and Jones, R.D. (1989). Successful treatment of a harlequin fetus. Arch. Dis. Child. 64, 1309–1311.

23. Menne, T., Larsen, U., Veien, N., Klemp, P., and Branebjerg, P. (1989). 5-aminosalicylic acid in a cream base improves psoriasis. A double-blind study. J. Dermatolog. Treat. 1, 5–7.

24. Jorgensen, A.P., and Menne, T. (1988). Aminosalicylic-acid derivatives for the treatment of psoriasis. US patent EP0291159A3, filed March 31, 1988, and granted November 17, 1988.

25. Hurwitz, E.S. (1989). Reye's syndrome. Epidemiol. Rev. 11, 249–253.

26. Chapman, J., and Arnold, J.K. (2020). Reye Syndrome (Statpearls).

27. Paine, D. (1958). Fatal hepatic necrosis associated with aminosalicylic acid; review of the literature and report of a case. JAMA 167, 285–289.

28. Khokhar, O.S., and Lewis, J.H. (2010). Hepatotoxicity of agents used in the management of inflammatory bowel disease. Dig. Dis. 28, 508–518.

29. Winter, H.S., Krzeski, P., Heyman, M.B., Ibarguen-Secchia, E., Iwanczak, B., Kaczmarski, M., Kierkus, J., Kolaček, S., Osuntokun, B., Quiros, J.A., et al. (2014). High- and low-dose oral delayed-release mesalamine in children with mild-to-moderately active ulcerative colitis. J. Pediatr. Gastroenterol. Nutr. 59, 767–772.

30. Furin, J., Brigden, G., Lessem, E., and Becerra, M.C. (2013). Novel pediatric delivery systems for second-line anti-tuberculosis medications: a case study. Int. J. Tuberc. Lung Dis. 17, 1239–1241.

31. Rajpopat, S., Moss, C., Mellerio, J., Vahlquist, A., Gånemo, A., Hellstrom-Pigg, M., Ilchyshyn, A., Burrows, N., Lestringant, G., Taylor, A., et al. (2011). Harlequin ichthyosis: a review of clinical and molecular findings in 45 cases. Arch. Dermatol. 147, 681–686.

32. Murray, J.F., Schraufnagel, D.E., and Hopewell, P.C. (2015). Treatment of tuberculosis. A historical perspective. Ann. Am. Thorac. Soc. 12, 1749–1759.

33. Rousseaux, C., El-Jamal, N., Fumery, M., Dubuquoy, C., Romano, O., Chatelain, D., Langlois, A., Bertin, B., Buob, D., Colombel, J.F., et al. (2013). The 5-aminosalicylic acid antineoplastic effect in the intestine is mediated by PPARγ. Carcinogenesis 34, 2580–2586.

34. Allgayer, H. (2003). Review article: mechanisms of action of mesalazine in preventing colorectal carcinoma in inflammatory bowel disease. Aliment. Pharmacol. Ther. 18 (Suppl 2), 10–14.

35. Mao-Qiang, M., Fowler, A.J., Schmuth, M., Lau, P., Chang, S., Brown, B.E., Moser, A.H., Michalik, L., Desvergne, B., Wahli, W., et al. (2004). Peroxisome-proliferator-activated receptor (PPAR)-gamma activation stimulates keratinocyte differentiation. J. Invest. Dermatol. 123, 305–312.

36. Schmuth, M., Haqq, C.M., Cairns, W.J., Holder, J.C., Dorsam, S., Chang, S., Lau, P., Fowler, A.J., Chuang, G., Moser, A.H., et al. (2004). Peroxisome proliferator-activated receptor (PPAR)-beta/delta stimulates differentiation and lipid accumulation in keratinocytes. J. Invest. Dermatol. 122, 971–983.

37. DiTommaso, T., Cottle, D.L., Pearson, H.B., Schlüter, H., Kaur, P., Humbert, P.O., and Smyth, I.M. (2014). Keratin 76 is required for tight junction function and maintenance of the skin barrier. PLoS Genet. 10, e1004706.

38. Magcwebeba, T., Riedel, S., Swanevelder, S., Bouic, P., Swart, P., and Gelderblom, W. (2012). Interleukin-1α Induction in Human Keratinocytes (HaCaT): An In Vitro Model for Chemoprevention in Skin. J. Skin Cancer 2012, 393681.

39. Cogen, A.L., Walker, S.L., Roberts, C.H., Hagge, D.A., Neupane, K.D., Khadge, S., and Lockwood, D.N. (2012). Human beta-defensin 3 is up-regulated in cutaneous leprosy type 1 reactions. PLoS Negl. Trop. Dis. 6, e1869.

40. Di Paolo, M.C., Merrett, M.N., Crotty, B., and Jewell, D.P. (1996). 5-Aminosalicylic acid inhibits the impaired epithelial barrier function induced by gamma interferon. Gut 38, 115–119.

41. Hsia, E., Johnston, M.J., Houlden, R.J., Chern, W.H., and Hofland, H.E. (2008). Effects of topically applied acitretin in reconstructed human epidermis and the rhino mouse. J. Invest. Dermatol. 128, 125–130.

42. Cottle, D.L., Kretzschmar, K., Schweiger, P.J., Quist, S.R., Gollnick, H.P., Natsuga, K., Aoyagi, S., and Watt, F.M. (2013). c-MYC-induced sebaceous gland differentiation is controlled by an androgen receptor/p53 axis. Cell Rep. 3, 427–441.

43. Chen, E.Y., Tan, C.M., Kou, Y., Duan, Q., Wang, Z., Meirelles, G.V., Clark, N.R., and Ma'ayan, A. (2013). Enrichr: interactive and collaborative HTML5 gene list enrichment analysis tool. BMC Bioinformatics 14, 128.

STAR★METHODS

KEY RESOURCES TABLE

REAGENT or RESOURCE	SOURCE	IDENTIFIER
Antibodies		
Anti-ABCA12	Sigma Aldrich	HPA078239; RRID:AB_2732373
anti-Involucrin	Covance	PRB-140C; RRID:AB_291569
anti-Keratin 6a	Covance	PRB-169P; RRID:AB_10063923
anti-Keratin 6a	Biolegend	905701 (formerly PRB-169P)
anti-Keratin 10	Covance	PRB-159P; RRID:AB_291580
anti-Keratin 10	Santa Cruz Biotechnology	RKSE60; sc-23877; RRID:AB_2134668
anti-Keratin 14	Abcam	LL002; ab7800; RRID:AB_306091
anti-Loricrin	Covance	PRB-145P; RRID:AB_10064155
anit-Periplakin	Abcam	ab72422; RRID:AB_1269719
Chemicals, Peptides, and Recombinant Proteins		
5-aminosalicylic acid (5ASA)	Sigma-Aldrich	PHR1060, A3537
4-aminosalicylic acid (4ASA)	Sigma-Aldrich	A79604
Prednisolone	Sigma-Aldrich	P6004
Ibuprofen	Sigma-Aldrich	I4883
4-hydroxytamofixen (4OHT)	Sigma-Aldrich	H6278
AD Cream	Johnson and Johnson	Aveeno Dermexa Moisturising Cream
Acitretin	Sigma-Aldrich	44707
Aspirin	Sigma-Aldrich	A2093
Critical Commercial Assays		
Quantibody Mouse Inflammation Array Q1 kit	RayBiotech	QAM-INF-1-1
Experimental Models: Organisms/Strains		
Mouse: Abca12^{lx12}: Abca12^{tm1Lex}	Lexicon Genetics	NIH-0129
Mouse: Abca12^{fl/fl}: Abca12^{tm1a(EUCOMM)Hmgu}	EUCOMM	*Abca12^{tm1a(EUCOMM)Hmgu}*
Mouse: B6Flpe: Gt(ROSA)26Sor^{tm1(FLP1)Dym}	WEHI	Tg(CAG-flpe)2Arte
Mouse: K14CreER: Tg(KRT14-cre/ERT)20Efu	Elaine Fuchs	Tg(KRT14-cre/ERT)20Efu
Oligonucleotides		
Lx12 genotyping	Wild type allele	F 5′CAGCTGCATGCGGCGATCAC
Lx12 genotyping	Wild type allele	R 5′CATGCGTGCGTTGAAT
Lx12 genotyping	Recombined allele	F 5′GGATTGGGAAGACAATAGCAGG
Lx12 genotyping	Recombined allele	R 5′CTTGGCAGAGTACATCTCAG
Abca12 tm1a	Wild type and tm1a alleles	5′ CATCGGTCCCACTGTGTTCCTGG (P1)
Abca12 tm1a	Wild type and tm1a alleles	5′ GAAAACAGAAACAAGGCCTGC (P2)
Abca12 tm1a	Wild type and tm1a alleles	5′ CAACGGGTTCTTCTGTTAGTCC (P3)
Abca12 tm1a	Wild type and floxed alleles	5′ CATCGGTCCCACTGTGTTCCTGG (P1)
Abca12 tm1a	Wild type and floxed alleles	5′ GAAAACAGAAACAAGGCCTGC (P2)
Abca12 tm1a	Wild type and floxed alleles	5′ ATGCAGAAGGTTCAGGGCTCC (P4)
Abca12 tm1a	Wild type and recombined alleles	5′ CATCGGTCCCACTGTGTTCCTGG (P1)
Abca12 tm1a	Wild type and recombined alleles	5′ GAAAACAGAAACAAGGCCTGC (P2)
Abca12 tm1a	Wild type and recombined alleles	5′ AGAAGCCCACAGCTCAAAGATGA (P5)

RESOURCE AVAILABILITY

Lead Contact

Further information and requests for resources and reagents should be directed to and will be fulfilled by the Lead Contact, Ian Smyth (ian.smyth@monash.edu).

Materials Availability
This study did not generate unique reagents.

Data and Code Availability
This study did not generate datasets other than those presented in the manuscript.

EXPERIMENTAL MODEL AND SUBJECT DETAILS

Abca12^{tm1Lex} NIH-0129 (*Abca12^{lx12}*) knockout mice were from Lexicon Genetics and have been described previously.[5] Embryonic stem cells targeted with the *Abca12$^{tm1a(EUCOMM)Hmgu}$* allele (*Abca12^{tm1a}*) were sourced from EUCOMM/KOMP and viable animals generated with the services of the Australian Phenomics Network and Monash Genome Modification Platform (MGMP). The *Abca12 ^{flox}* conditional allele was produced by crossing *Abca12^{tm1a}* mice with B6Flpe mice expressing a germline flippase which excised the LacZ gene trap reporter cassette leaving a floxed conditional allele. The B6Flpe transgene was then removed through selective breeding. *Abca12$^{f/f}$;K14-CreER* mice were generated by cross breeding.[14] All animal procedures complied with standards set under Australian guidelines for animal welfare and experiments were subject to Monash University animal welfare ethics review panels. All animals were maintained on a C57BL6/J background. Animals were co-housed in Specific Pathogen Free (SPF) conditions. Animals were randomly assigned to experimental groups according to genotype. Both male and female embryo/mice were used in all experiments in approximately equal numbers.

METHOD DETAILS

Genotyping
Abca12 Lx12 genotyping was performed with primer pair 5′CAGCTGCATGCGGCGATCAC and 5′CATGCGTGCGTTGAAT for the *Abca12 wild-type* allele and primer pair 5′GGATTGGGAAGACAATAGCAGG and 5′CTTGGCAGAGTACATCTCAG for the *Abca12 lx12* allele. *Wild-type* bands ran at 507bp and *Lx12* at 272bp. *Lx12* PCRs where performed using a HOTstart method with Taq polymerase (NEB). Cycling parameters were, initial denaturation at 95°C for 3 mins, followed by 2 cycles of denature 95°C for 30 s, anneal 65°C for 30 s, extension 72°C for 45 s, 35 cycles of denature 95°C for 30 s, anneal 63°C for 30 s, extension 72°C for 45 s and a final polishing extension cycle of 72°C for 10 minutes.

K14-CreER and internal control genotyping was performed as described elsewhere.[37] The PCR for the *Abca12 tm1a* allele used primer trio 5′ CATCGGTCCCACTGTGTTCCTGG (P1), 5′ GAAAACAGAAACAAGGCCTGC (P2) and 5′ CAACGGGTTCTTCTGTTAG TCC (P3), where the ~180bp product of primers P1 and P2 detects the wild-type allele and the ~300bp product of primers P1 and P3 detects the *Abca12 tm1a* allele. To detect the *Abca12 floxed* allele (after flippase recombination) and wild-type allele, the primer pair P1 and 5′ ATGCAGAAGGTTCAGGGCTCC (P4) where used. Bands run at ~580bp and ~480bp respectively. To detect the *Abca12 delta* allele, the primer pair P1 and 5′ AGAAGCCCACAGCTCAAAGATGA (P5) were used. The *Abca12 delta* band runs at 435bp while the *Abca12 floxed* and *wild-type* alleles are also detected as larger bands of 1220bp and 1051bp respectively. PCRs where performed using a HOTstart method with REDExtract-N-Amp PCR reaction mix (Sigma-Aldrich). Cycling parameters were, initial denaturation at 94°C for 3 mins, followed by 35 cycles of denature 94°C for 30 s, anneal 59°C for 30 s, extension 72°C for 45-90 s and a final polishing extension cycle of 72°C for 5 minutes.

Embryonic skin culture
Embryos were harvested at E16.5 under sterile conditions and cultured *ex-vivo*. The mid to lower back skin was isolated and cut into left and right-side halves and cultured dermis-side down on 6 well chamber inserts (Costar Transwell Permeable supports CLS3450-24EA). One skin section of each matched pair was grown at 37 degrees with 1.5ml of DMEM supplemented with 10% FCS, P/S and L-Glutamine media added to the lower chamber while the other was grown in media containing 10mM 5-aminosalicylic acid (5ASA) (Sigma-Aldrich PHR1060) or 10mM 4-aminosalicylic acid (4ASA) (Sigma-Aldrich A79604), forming an air-liquid interface with the dermis drawing media from the lower chamber while the epidermis remained dry. In other experiments 0.1 μM Prednisolone, and 1.25mM Ibuprofen were trialled.[38–40] Respective media was changed after 48 hours and skin cultures harvested after 96 hours of culture. The skin was then cut from chamber inserts leaving membrane backing intact for support during 4 hours of fixation with 4% PFA at room temperature. Samples were finally stored in 70% ethanol and membrane backing removed before being processed for paraffin histology using standard methods.

Tamoxifen induction of HI
Mice were aged to between 7-9wks when the hair cycle is in telogen. The lower back was clipped to remove hair and expose a region of skin above the tail of approximately 3-5cm^2 (treatment site). Mice were then dosed with 1.5mg of 4-hydroxytamofixen (4OHT) (Sigma-Aldrich H6278-50MG) in 0.1ml of acetone applied dropwise by pipette to the treatment site and this was repeated 2 and 4 days later to induce gene deletion and trigger HI. Mice were monitored, weighed daily and given access to wet diets (Wombaroo powder, soaked pellets, and nectar jelly) in addition to dry diets of Barastoc rodent chow and sunflower seeds. Both males and females were used, as gender did not affect the HI phenotype. Mice were predominantly culled on day 11. Mice that were occasionally

culled prematurely due to poor health have been excluded from day 11 end point analysis. The treatment region skin was collected, flattened onto nitrocellulose membrane and cut into strips. Some strips were then fixed in 10% NBF overnight. Samples were then stored in 70% ethanol and membrane backing removed before being processed for paraffin histology using standard methods. Alternatively, additional skin strips were peeled from the backing membrane and snap frozen in liquid nitrogen then stored at −80 degrees for RNA extraction and Nanostring analysis.

5ASA intraperitoneal injection

Mice were fitted with Elizabethan collars (Lomir) under isoflurane to limit 4OHT oral exposure. Collars were removed on day 5 and starting day 5 until day10 mouse cohorts were treated once daily (for 6 days) by intraperitoneally injecting 5-ASA daily at 25mg/kg and 125mg/kg using the protocol and vehicle of Sudheer Kumar et al.[16] Mice were predominantly culled on day 11. Mice that were occasionally culled prematurely due to poor health have been excluded from day 11 end point analysis.

Topical application of creams

Mice were fitted into butterfly harnesses (Lomir) under isoflurane to limit grooming of treatment site (and reduce ingestion of treatment compounds) for as long as tolerated. Harnesses were adjusted and refitted as needed and removed when reaching ∼13% weight loss. Starting from day 5 until day 10, mouse cohorts were treated once daily (for 6 days) with 0.1ml of 3 or 6% (w/w) 5ASA, 0.02% (w/w) Acitretin, combination of 0.02% (w/w) Acitretin and 3% (w/w) 5ASA, 3% (w/w) Aspirin, 3% (w/w) 4ASA, or 1.5% (w/w) 4ASA mixed into Aveeno Dermexa Moisturizing Cream (Johnson and Johnson), or AD cream alone rubbed with a cotton tip into the treatment site. Starting 5ASA dosage was determined empirically but found to be similar to that of psoriasis trials.[23] Creams containing 0.02% Acitretin showed efficacy in prior mouse skin studies.[41]

Assay of urine salicylic acid content

Urine was collected from mice at death and stored at −80°C. Analysis of salicylic acid content in urine was performed based on the original Trinder protocol.[17] Briefly, Trinder color reagent was prepared as 40 g Mercuric Chloride, 120ml 1M HCl, 40 g Ferric Nitrate dissolved to 1L in distilled water. Urine was diluted 1:5 in distilled water and 20 μL of dilute urine added to 0.1ml of Trinder color reagent. The color intensity was read with a plate reader at 540nm and calibrated against a standard curve from 0 to 0.6mg/ml of salicylic acid. Sample concentration was determined from the standard curve and corrected for the dilution factor. Values are expressed as a relative fold change with the Salicylic acid content of urine from day 11 untreated *Abca12*$^{f/f}$ mice arbitrarily defined as 1. Control urine samples spiked with known quantities of Salicylic acid demonstrated a 98% detection rate for the assay.

Histological Analysis and Microscopy

Tissues were paraffin imbedded and sectioned at 8 μm. Antigen retrieval was performed in Citrate buffer pH6 using Tefal pressure cooker. Antibody staining was performed as described elsewhere,[42] and coverslips mounted using Prolong Gold (Invitrogen). Imaging was using an Olympus Fluoview 500 confocal microscope (Biochemistry Imaging Suite).

Antibodies and immunostaining

Anti-ABCA12 1:500 (HPA078239) (IHC-IF) Sigma-Aldrich, Germany. anti-Filaggrin (PRB-417P) 1:1000 (IHC-IF) Covance, USA. anti-Involucrin (PRB-140C) 1:1000 (IHC-IF) Covance, USA. Anti-Keratin 6a (PRB-169P) 1:500 (IHC-IF) Covance, USA replaced by (905701) 1:2500 (IHC-IF) Biolegend, USA. anti-Keratin 10 (PRB-159P) 1:500 (IHC-IF) Covance, USA. antiKeratin 10 (RKSE60) (sc-23877) 1:100 (IHC-IF) Santa Cruz Biotechnology Inc, USA. anti-Keratin 14 (LL002) (ab7800) 1:250-1000 (IHC) Abcam, UK. anti-Loricrin (PRB-145P) 1:1000 (IHC-IF) Covance, USA. Anti-Periplakin (ab72422) 1:200-500 (IHC-IF) Abcam, UK. Alexa Fluor® A488/555 secondary antibodies raised in Donkey, against rabbit/mouse, were used at 1:600, from Invitrogen. Nuclei stains were DAPI 1mg/ml (Sigma) 1:250-1000. LacZ staining was performed as previously described.[37]

Nanostring mRNA Analysis

RNA was extracted from snap frozen skin tissue (∼0.5cm^2 area) using QiaShredders in conjunction with QIAGEN RNAeasy Mini Kits according to manufacturer's protocol. Tissue was initially crushed using eppy pestles in RLT Buffer and during this procedure the epidermis disintegrated and disassociated from the dermis. The intact dermis did not pass the Qiashredder and was discarded to leave epidermis enriched RNA. mRNA analysis was performed using custom Nanostring probes of GX codeset chemistry (See SI excel file), according to the manufacturers protocol on a nCounter SPRINT Profiler. Raw counts were exported from nSolver 4.0 software and analyzed in excel. All mRNA was normalized to housekeeping gene *Edc3* and expressed relative to untreated control mice. Tables showing significant gene changes (Data S1) comparing untreated and test conditions, have been filtered to remove genes found to be similarly changed when comparing untreated and vehicle/carrier conditions and so only reflect drug-dependent changes. Likewise, significantly changed genes found commonly changed between untreated and test conditions, and vehicle and test conditions, have been removed to avoid duplication with vehicle versus test condition tables. Heatmaps were created using https://discover.nci.nih.gov/cimminer/home.do Venn diagrams were created using Venny 2.1 https://bioinfogp.cnb.csic.es/tools/venny/. GO and MGI mammalian phenotype analysis performed with Enricher https://maayanlab.cloud/Enrichr3/.[43] Gene profiles were

also analyzed using Ingenuity Pathway Analysis (IPA) software (QIAGEN) for downstream pathway predictions on default settings. Changes in Z-scores greater than 2 (or less than −2) were considered the threshold for significant predictions.

Inflammatory Array

Protein lysates were extracted from snap frozen skin tissue (∼0.5cm^2 area) by homogenizing in 200 μL of 0.25% NP-40 in Tris Buffered Saline ph 7.2-7.5 (extraction buffer) and rocking at 4°C for 2 hours. The supernatant fraction was then collected by spinning at 16,000rpm in an Eppendorf tube centrifuge for 10 minutes at 4°C, then stored at −80°C until used. Protein concentration was determined using a BioRad DC reagent kit according to manufacturer's protocol. Analysis of inflammatory factors was performed using a 40 factor RayBiotech Quantibody Mouse Inflammation Array Q1 kit (QAM-INF-1-1) according to manufacturer's protocol. Protein extracts were standardized to 2.5-5mg/ml in extraction buffer then diluted 5-fold in sample diluent buffer (RayBiotech) to final 0.5-1mg/ml concentration. Fluorescent was detected with a Genepix 4000B slide scanner and intensity determined with Genepix software using RayBiotech Quantibody Mouse Inflammation Array Q1 gal file. Analysis was then performed using the RayBiotech Quantibody Mouse Inflammation Array Q1 Excel tool.

Transepidermal water loss assays

Assays were performed using embryonic skins grown in *ex vivo* cultures with and without 10mM 4ASA for 4 days as outlined previously. Skins were removed from chamber membranes and each placed onto glass coverslips with Vaseline applied to seal the edge of the skin segments. An image was taken with a ruler to calculate skin surface area and each skin coverslip weighed to determine starting weight. Skins were left at room temperature exposed to the open air to dry. Weights were measured at 30, 60, 120, 180, 240, 300, 360 minutes to determine evaporative weight loss in mg. Changes in weight were then adjusted relative to the skin surface area in cm^2 to determine TEWL.

QUANTIFICATION AND STATISTICAL ANALYSES

All thickness quantification was carried out using ImageJ (Java) software. Data throughout this study was analyzed by the unpaired Student's t test assuming unequal variance, also known as Welch t test, except for TEWL assays which used a paired Student's t test.